Imaging of Traumatic Carpal Instability

J.-C. Dosch and T. Moser

Ligaments of the wrist play a fundamental role in the stability of the carpus. Poirier and Charpy [1] and Testut [2] first described this relationship. The works of Mayfield et al. [3] and Taleisnik [4] constitute the basis of the current description. More recently, Berger [5] has contributed some modifications to this classification. Classically, we differentiate between intra-articular or interosseous ligaments and capsular ligaments. The latter group is further classified into intrinsic ligaments, which originate and insert into carpal bones, and extrinsic ligaments, which attach carpal bones to bones of the forearm or the hand [6].

1 Classification of Instability

The classification of carpal instability is complex and variable according to the authors. Larsen proposes an analysis of carpal instability according to six criteria: the duration of evolution, permanent radiographic signs, aetiology, topography, direction and mechanism [7].

J.-C. Dosch (✉)
Hand Surgery Unit, Service de Radiologie, CHU Strasbourg, Hôpital de Hautepierre, Avenue Molière, Strasbourg, Cedex 67098, France

Centre de Chirurgie Orthopédique et de la Main Illkirch, BP 49, Strasbourg, Cedex 67098, France
e-mail: jean-claude.dosch@chru-strasbourg.fr

T. Moser
Département de Radiologie, CHUM, Hôpital St Luc, 1058 rue St Denis, Montréal, QC H2X 3J4, Canada
e-mail: thomas.moser@umontreal.ca

E. Camus, L. Van Overstraeten (eds.), *Carpal Ligament Surgery*,
DOI 10.1007/978-2-8178-0379-1_4, © Springer-Verlag France 2013

- Duration: acute being less than 1 week, subacute 1–6 weeks or chronic over 6 weeks. This influences healing of lesions.
- The permanence of the instability is correlated to the severity of the ligamentous lesion. *Static* instability is permanent and visible on static x-rays, whereas *dynamic* instability is only detected on certain movement patterns and is demonstrated only on dynamic radiography (under fluoroscopy). *Predynamic* instability is a subtle anomaly nonapparent on radiography.
- Aetiology is mostly traumatic but may also be congenital or rheumatoid.
- The topography may concern the radiocarpal joint, the proximal row, the midcarpal joint, the distal row or the carpometacarpal joint.
- Directions are variable. Dorsal instability or 'dorsal intercalated segment instability – DISI' is the most common. The lunate is tilted into dorsal flexion and translated anteriorly. The ulnar translation and dorsal subluxation correspond to the sliding of the carpus on the radial slope, medially and posteriorly. We distinguish between type I ulnar translation when the carpus is shifted interiorly and type II when the scaphoid remains in place due to a scapholunate diastasis [6].
- There are several mechanisms. In 'dissociative carpal instability – DCI', there is an imbalance between bones of the same row. The main causes are scaphoid fracture, scapholunate or lunotriquetral ligament rupture [8, 9]. In 'nondissociative carpal instability – NDCI', the instability is radiocarpal (between radius and first carpal row) or midcarpal (between first and second carpal rows). In 'complex carpal instability', elements of both types DCI and NDCI are present. 'Adaptative carpal instability – ACI' is a defect of alignment following an extrinsic anomaly often an epiphyseal nonunion of the radius [10].

2 Mechanisms of Intracarpal Ligament Lesions

2.1 Lesions of the Ligaments of the Radial Side of the Wrist

The mechanism of these traumatic wrist lesions is stereotyped, almost always a fall on the outstretched hand. When the arm is abducted, impact on the thenar eminence induces extension, ulnar deviation and intracarpal supination of the wrist. These displacements are particularly deleterious to the radial ligaments of the wrist.

2.2 Progressive Perilunate Instability

According to Mayfield, this mechanism is the origin of the perilunate instability classification, which is progressive in gravity in function of the energy of the trauma and the number of ligaments ruptured [11]. Pure ligamentous lesions follow the lesser arc of Johnson, first involving the scapholunate junction (scapholunate ligament rupture, stage 1), then the capitolunate junction (rupture of radioscaphocapitate ligament, stage 2), lunotriquetral (stage 3) and radiolunate (rupture of the dorsal radiocarpal ligament, stage 4), leading to the palmar tilt of the lunate [12]. As the energy increases further, lesions progressively involve carpal bones along the greater arc of Johnson, giving the classification table for fracture palmar subluxations of the lunate [13].

2.3 Progressive Scaphoid Instability

Watson described the evolution of scapholunate lesions [14, 15]. Stage 1 is a dorsal carpal syndrome – synovitis of the scapholunate interval with moderate ligament injury. Pain is primarily on activity (especially with racquet sports) and its persistence at rest is a sign of aggravation. There is tenderness on the dorsal scapholunate interval and finger extension test is positive.

2.4 Rotatory Scaphoid Subluxation (RSS)

This involves more severe ligament injuries causing dorsal displacement with rotation of the proximal pole. The abnormal forces on the radioscaphoid joint cause ‘scapholunate advanced collapse SLAC’ wrist [16]. There are symptoms of at least 6 months’ duration with pain at rest and limitation of range of motion, especially flexion. Tenderness over the scaphoid or on Watson’s test is elicited on examination. Watson described five types of RSS. Predynamic RSS (type 1) involves clinical instability with no radiographic abnormality.

Dynamic RSS (type 2): Radiographic abnormality only on stress views: scaphoid shortening with ring sign, superposition of the scaphoid and capitate.

Static RSS (type 3): More severe clinical abnormality and radiographic abnormalities in neutral position: scapholunate gap, increased scapholunate angle with or without DISI. This can be reducible or non-reducible.

Degenerative stage (type 4) or ‘SLAC’ wrist develops after prolonged evolution. X-rays show radioscaphoid followed by capitolunate arthritis.

The last type of RSS (type 5) is *secondary* to other carpal lesions such as primary necrosis of the lunate (Kienbock’s disease) or the scaphoid (Preiser’s). When it complicates scaphoid nonunion, it is known as ‘scaphoid nonunion advanced collapse – SNAC’ wrist.

3 Ulnar-Sided Lesions

Lunotriquetral ligament rupture is encountered in two cases. The first is radial-sided wrist injury as in Mayfield stage 3 where it passes to the next level. Isolated lunotriquetral ligament rupture can occur in ulnar-sided wrist trauma where the mechanism of injury is similar but with arm adduction causing ulnar impact. Trauma to the hypothenar eminence causes extension, radial inclination and intracarpal pronation.

With respect to the Mayfield theory, Viegas et al. described the reversed perilunate instability [17]. Lunotriquetral ligament rupture presents clinically with ulnar-sided wrist pain which is exacerbated by compression tests and lunotriquetral ballottement. X-rays show lunotriquetral diastasis and lunate tilt in VISI.

4 Standard Radiography

Four views are required in any wrist trauma: posteroanterior, lateral, oblique and scaphoid views [18]. Posteroanterior palm down and lateral views are sufficient to show the essential wrist landmarks for assessment of instability. Success criteria for the PA view are (Fig. 1):

1. A continuity between the medial cortex of the ulna and the ulnar styloid
2. ECU gutter in the middle of the fossa [19]

For the lateral view, the criteria are (Fig. 2):

1. Superposition of the radius and ulna
2. Pisiform projects between the anterior cortex of the capitate posteriorly and the distal pole of the scaphoid anteriorly [20]

On these views, we can note:

- Carpal arches described by Gilula to assess the alignment of the two carpal rows. The first arch is formed by the superior convex border of the scaphoid, lunate and triquetrum and the second by their concave borders. The third arch is formed by the proximal borders of the capitate and hamate [21]. These arches delineate harmonious curves in neutral position. In radial or ulnar deviation, we can observe physiological abutment [22].

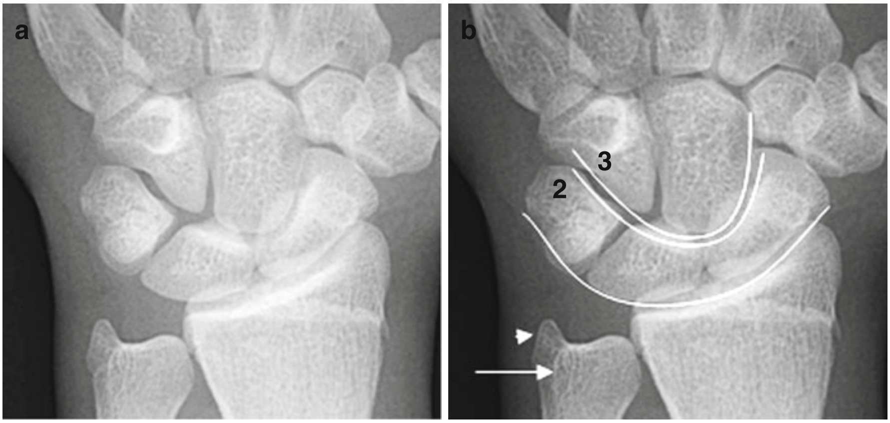

Fig. 1 PA view in neutral position. (**a**) Without marking, (**b**) with marking. Harmonious three Gilula arches, ulnar styloid in the extension of the medial ulnar cortex (*arrow head*), extensor carpi ulnaris groove in relation to fossa (*white arrow*) suppress **2** and **3**

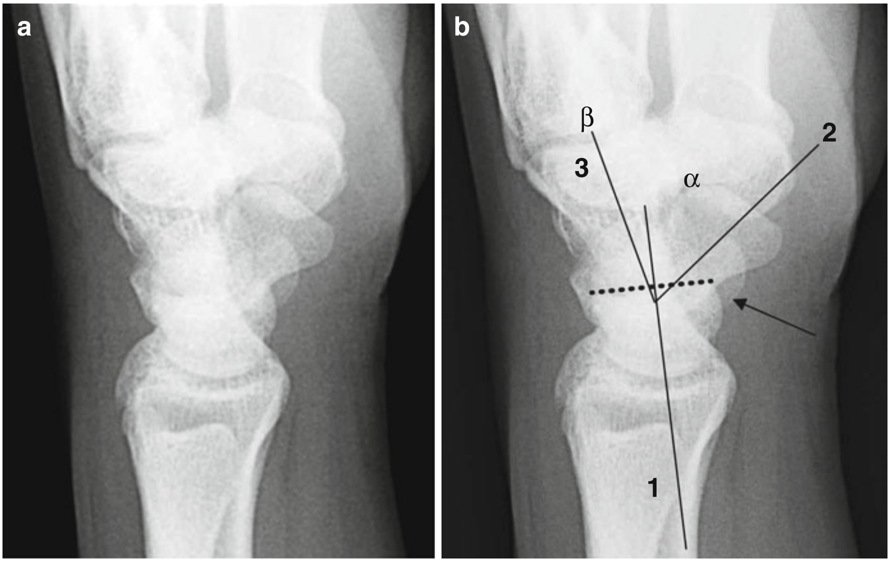

Fig. 2 Lateral view in neutral position. (**a**) Without marking, (**b**) with marking: Superposition of the radius and ulna. Pisiform between scaphoid tubercle and anterior facet of capitate (*arrow*). Lunate axis (*line 1*) perpendicular to the line connecting the anterior and posterior horns (*dotted line*). Scaphoid axis (*line 2*). Capitate axis (*line 3*). Scapholunate *angle alpha*. Capitolunate *angle beta*

- The regularity of these lines (on PA).
- All lines do not normally exceed 3 mm thickness. The opposing articular surfaces are parallel, and in the absence of flexion, any overriding indicates the presence of a fracture or subluxation. The scapholunate space must be carefully scrutinized. In fact, in the axial plane, this interval is parallel in only 80 % and divergent with respect to the anterior and posterior horns of the lunate in 15 % of cases [23]. Thus, the measure of this space must be taken at the middle. Scapholunate diastasis is considered if the interval exceeds 3 mm. This may be physiologic in lunotriquetral synostosis or inherent laxity (bilateral comparative x-rays are recommended), or pathologic in association to ligament rupture (Fig. 3) [24, 25].
- Carpal angles (lateral view).
- The lunate axis is defined by the line perpendicular to the tangent connecting the two horns of the lunate. The scaphoid axis passes through the centre of the tubercle, waist and base of the scaphoid. The axes of the radius and the capitate are calculated by dropping a perpendicular to the line connecting the two equidistant points on the anterior and posterior borders of these two bones. The normal scapholunate angle is between 30° and 70° with a mean value of 55°. It increases in extension instability (DISI) and decreases in flexion instability (VISI). The radiolunate and capitolunate angles range between −15° and +15°. They increase in DISI or VISI (Fig. 4). The theoretical collinearity of the axes of the radius, lunate, capitate and third metacarpal is actually rarely seen (only 11 % normal subjects).

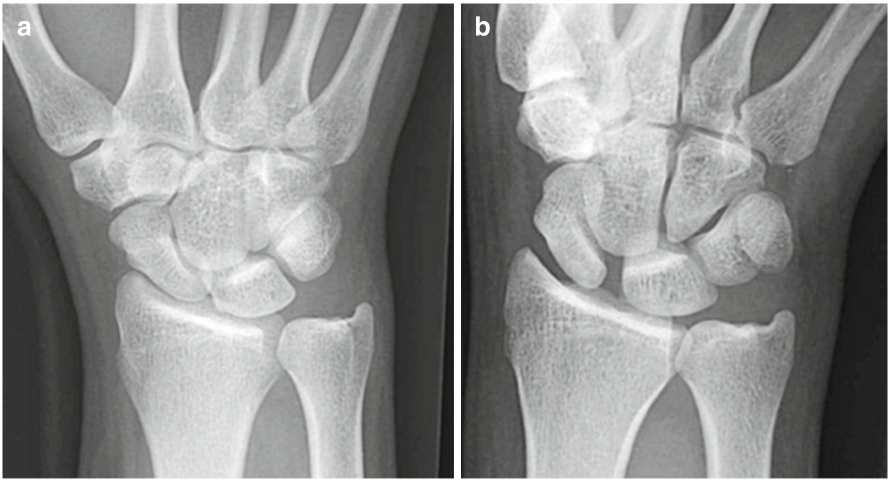

Fig. 3 Scapholunate diastasis. Scapholunate interval is not widened in neutral position (**a**). SL diastasis on AP view with 20° pronation (**b**)

The study of carpal dynamics is usually done to confirm clinical or radiographic suspicion of carpal instability. Gilula proposes PA views in neutral position, ulnar and radial deviation, a clenched fist PA view, lateral views in neutral position, flexion and extension. The clenched fist position increases intra-articular pressure and unmasks scapholunate diastasis [26]. Lawand proposes this test on both sides whilst clenching a pencil [27]. The interpretation of these views requires knowledge of the combined carpal movements in the sagittal and coronal planes (Fig. 5). In radial deviation, the first carpal row flexes. The scaphoid is shortened and shows the ring sign at its distal portion representing the tubercle seen escaping. The lunate follows the movement and appears triangular due to the displacement of its pointed posterior horn. In ulnar inclination, the first carpal row extends. The scaphoid elongates, exposing its waist. The lunate becomes quadrangular due to displacement of its rounded anterior horn which becomes more visible [28].

Radiography remains an investigation of low sensitivity. As repeatedly shown by experimental studies [29], the presence of radiographic signs of instability denotes extensive ligament lesions generally associated with complete or partial intrinsic and extrinsic ligaments, thus the need for complementary investigations [30].

To summarize:

1. Radiographic signs for DISI on PA view in neutral are scapholunate diastasis, superposition of the scaphoid and capitate, ring sign of the scaphoid, quadrangular shape of the lunate. On lateral view, they are the increase of scapholunate, capitolunate and radiolunate angles (Fig. 6).
2. Radiographic signs for VISI are decrease of scapholunate angle and increase of capitolunate and radiolunate angles.

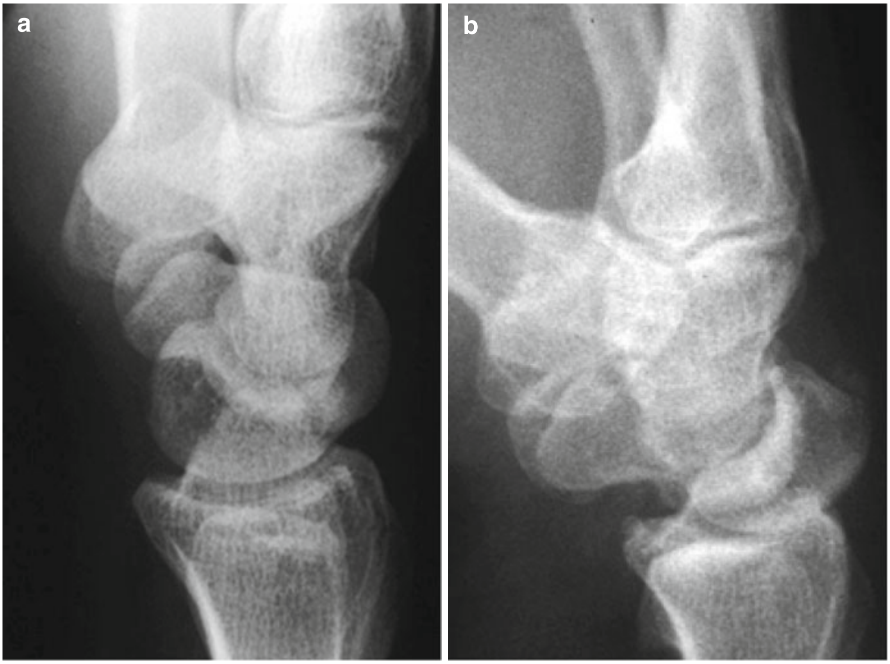

Fig. 4 Carpal instability. *DISI* dorsal tilt of the lunate and increased scapholunate angle, *VISI* ventral tilt of the lunate

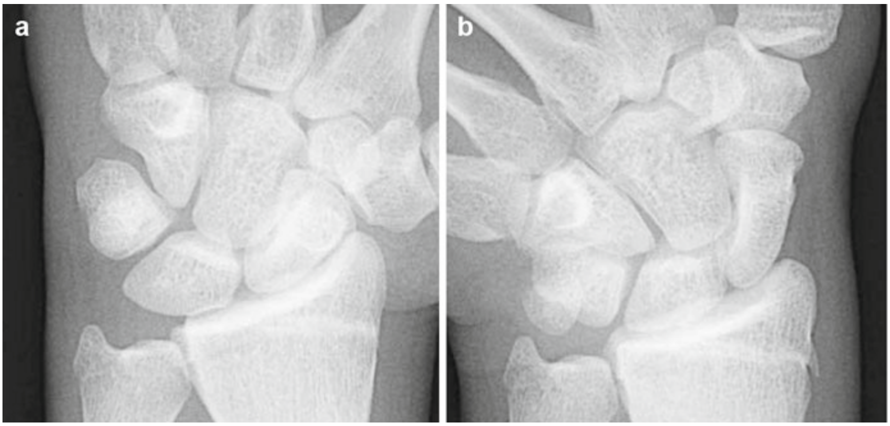

Fig. 5 Carpal dynamics in radial and ulnar inclination. (**a**) Radial inclination: The first carpal row is in flexion. The scaphoid is short and shows the ring sign. Triangular shape of the lunate is due to the pointed shape of its posterior horn. Physiological rupture of Gilula arch 1 regarding the lunotriquetral interval. (**b**) Ulnar inclination: The carpal bones are in extension. The scaphoid is elongated. Quadrangular shape of the lunate due to the large and rounded shape of its anterior horn

Fig. 6 Dorsal instability (DISI) at 1 month post traumatic. (**a**, **b**) Radiographs at day 0 showing no abnormality. (**c**, **d**) Control at 1 month shows a DISI. Pa shows shortened scaphoid with a ring sign, superposition of the scaphoid and capitate denoting rotational displacement, quadrangular lunate. Lateral view confirms the dorsal tilt of the lunate with a widening of the scapholunate angle

5 Ultrasound

The use of ultrasound for diagnosis of lesions of wrist ligaments is very recent [31–33]. It is an investigation of low sensitivity but high specificity which can be a useful cheap complement to the clinical examination. It requires, however, high-quality equipment with high-frequency ultrasound. The dorsal portion of the scapholunate ligament may be seen in most cases, the TFCC in one out of two cases and rarely, the dorsal portion of the lunotriquetral ligament. The interosseous ligaments are examined in transverse cuts from the dorsal side, whilst varying the degree of wrist flexion. The diagnosis of rupture depends on the appearance of the normal fibrous structure which is replaced by a zone of hypoechogenicity (Fig. 7) [34].

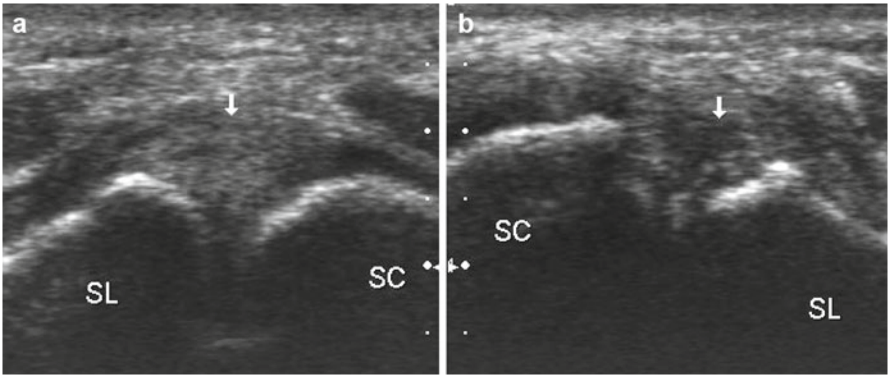

Fig. 7 Ultrasound of the scapholunate ligament. Comparative study of the dorsal portion; *SC* scaphoid, *L* lunate. (**a**) Normal SL (*arrow*), (**b**) Hypoechoic zone denoting rupture (*arrow*)

6 CT Scan

Simple CT scan without injection is not indicated in studying wrist ligaments. However, it shows associated osseous lesions perfectly.

7 MRI

Most studies use the 1.5 T system. A cadaveric study using a low-field machine showed limited results [35]. Several more recent studies compared the same sequences at 1.5 and 3.0 T [36–38]. The subjective quality and signal–noise relation was significantly higher at 3.0 T. The technical considerations of positioning are such that the wrist is seldom in a neutral position and thus the anatomical relations are modified. The most recent 3 T MRI study gives 100 % specificity and 89 and 82 % sensitivity for full-thickness scapholunate and lunotriquetral lesions, respectively [39].

8 Arthrography, Arthro-CT and Arthro-MRI

Opaque arthrography, notably triple arthrography with successive punctures of the midcarpal, radiocarpal and distal radioulnar joints, is but the precursor of CT or MR arthrography. The opacification of these compartments by contrast material – iodides for CT and gadolinium salts for the MRI – allows an exhaustive analysis of the different articular portions of the scapholunate and lunotriquetral ligaments.

The *scapholunate ligament* closes the proximal part of the interval. It is horseshoe-shaped and is formed of three anatomically and functionally distinct portions [40, 41]. The dorsal portion is short, transverse and trapezoidal. Composed of thick and tight collagen bands, it is the strongest part of the ligament. It forms the axis of

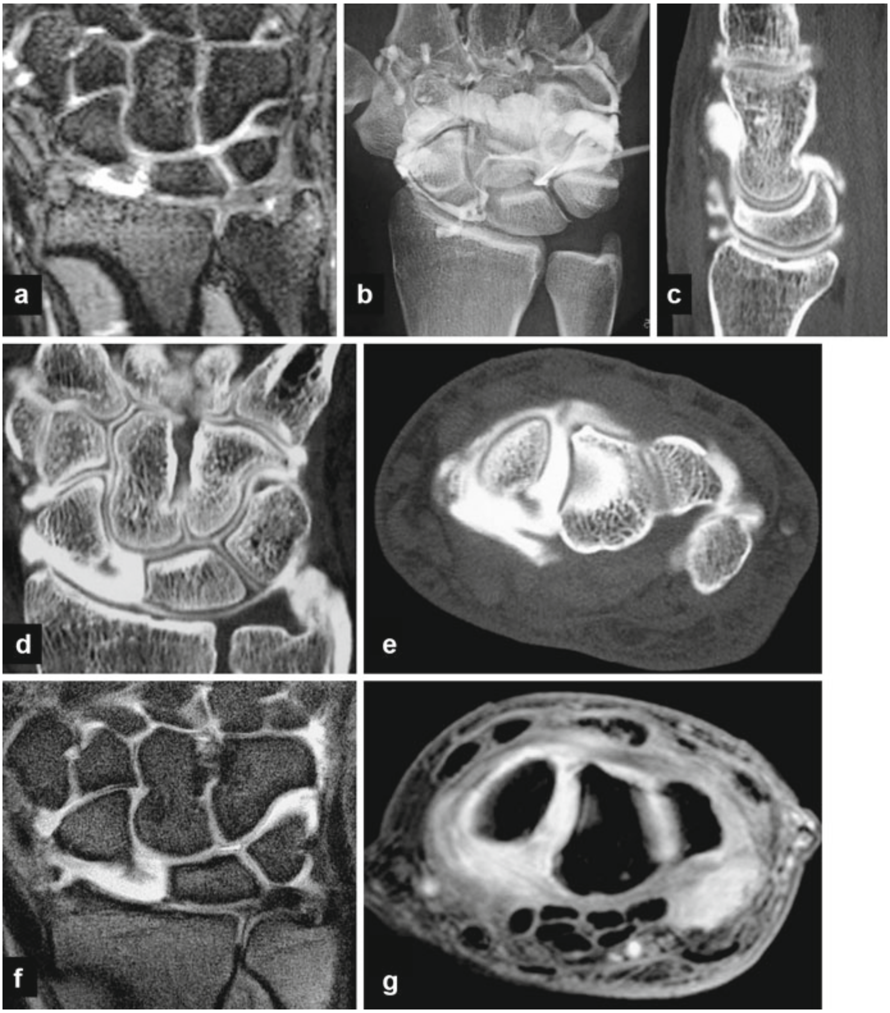

Fig. 8 Complete scapholunate ligament SLL rupture. (**a**) MRI shows scapholunate diastasis with ligament stump outlined by the effusion. (**b**) Midcarpal arthrography with contrast communicating to radiocarpal joint via incompetent SL interval. (**c**–**e**) CT arthrography showing the SLL stump and dorsal tilt of the lunate in DISI. (**f**–**g**) MR arthrography. The stump is less visible since soaked with contrast material

rotation between the scaphoid and the lunate. The proximal or intermediate portion resembles a meniscus with its triangular shape and fibrocartilaginous structure. It is proximally attached to the radioscapholunate facet and is the weakest part of the ligament. The palmar portion is long and slopes obliquely below and inwards. It is formed of finer and more loosely arranged collagen bands, allowing an anterior displacement of both bones in flexion. The scaphoid has a greater arc in flexion than the lunate due to a smaller curvature of its proximal pole.

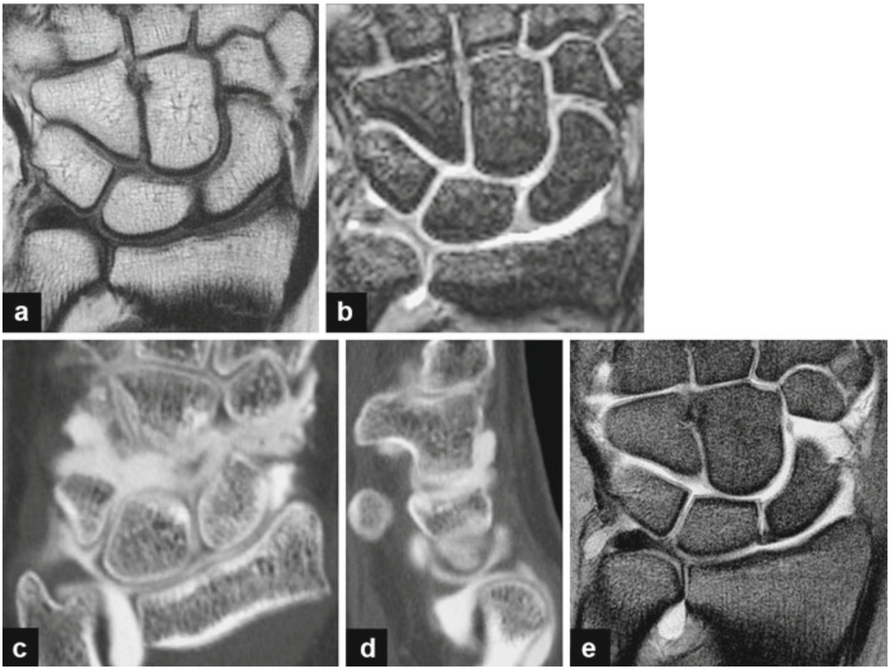

Fig. 9 Partial rupture of the LTL and central portion of the TFCC (type Palmer 2D). (**a**, **b**) MRI shows no visible abnormality. (**c**, **d**) CT arthrography shows the lesion perfectly in coronal and sagittal cuts. (**e**) MR arthrography shows no visible abnormality

The lunotriquetral ligament also has three portions [42, 43]. The dorsal portion is fibrous and is continuous with capsular ligaments posteriorly (radiocarpal and dorsal intracarpal). The proximal portion is fibrocartilaginous and meniscoid like. It is not very strong. The palmar portion is fibrous, strongest and most important functionally.

In arthro-CT [44] and arthro-MRI [30, 45, 46], the intermediate portions of these ligaments can be studied on coronal sections and the dorsal and palmar portions on axial sections. Ligamentous lesions are characterized by their extent and depth. Complete tear involves all three portions, whilst partial tears involve one or two, or even just a segment (punctuate ruptures) of the ligament (Figs. 8 and 9).

Full-thickness tears involve the entire thickness of the ligament whilst partial ones affect the palmar or dorsal aspect only without entailing articular communication. For full-thickness tears, it is important to determine whether the tear is central or peripheral (zone of insertion) for management plan. In a peripheral rupture, the stump retracts and appears thickened.

CT and MRI arthrography performance approaches actual arthroscopy. Associated lesions detected and analysed are primarily state of the cartilage and bone alterations and secondarily bone contusions and occult fractures.

References

1. Poirier P, Charpy A (1911) Traité d'Anatomie Humaine, vol 1. Masson et Cie, Paris
2. Testut L (1904) Traité d'Anatomie Humaine, vol 1. Octave Douin, Paris
3. Mayfield JK, Johnson RP, Kilcoyne RF (1976) The ligaments of the human wrist and their functional significance. Anat Rec 186(3):417–428
4. Taleisnik J (1976) The ligaments of the wrist. J Hand Surg Am 1(2):110–118
5. Berger RA (2001) The anatomy of the ligaments of the wrist and distal radioulnar joints. Clin Orthop 383:32–40
6. Taleisnik J (1988) Current concepts review. Carpal instability. J Bone Joint Surg Am 70(8):1262–1268
7. Larsen CF et al (1995) Analysis of carpal instability: I. Description of the scheme. J Hand Surg Am 20(5):757–764
8. Linscheid RL et al (1972) Traumatic instability of the wrist. Diagnosis, classification, and pathomechanics. J Bone Joint Surg Am 54(8):1612–1632
9. Wright TW et al (1994) Carpal instability non-dissociative. J Hand Surg Br 19(6):763–773
10. Brahin B, Allieu Y (1984) Compensatory carpal malalignments. Ann Chir Main 3(4):357–363
11. Mayfield JK (1984) Patterns of injury to carpal ligaments. A spectrum. Clin Orthop Relat Res 187:36–42
12. Mayfield JK (1984) Wrist ligamentous anatomy and pathogenesis of carpal instability. Orthop Clin North Am 15(2):209–216
13. Johnson RP (1980) The acutely injured wrist and its residuals. Clin Orthop Relat Res 149:33–44
14. Watson HK, Weinzweig J, Zeppieri J (1997) The natural progression of scaphoid instability. Hand Clin 13(1):39–49
15. Watson H, Weinzweig J (2001) The wrist. Lippincott Williams & Wilkins, Philadelphia, p 985
16. Watson HK, Ballet FL (1984) The SLAC wrist: scapholunate advanced collapse pattern of degenerative arthritis. J Hand Surg Am 9(3):358–365
17. Viegas SF et al (1990) Ulnar-sided perilunate instability: an anatomic and biomechanic study. J Hand Surg Am 15(2):268–278
18. Gilula LA et al (1984) Roentgenographic diagnosis of the painful wrist. Clin Orthop Relat Res 187:52–64
19. Levis CM, Yang Z, Gilula LA (2002) Validation of the extensor carpi ulnaris groove as a predictor for the recognition of standard posteroanterior radiographs of the wrist. J Hand Surg Am 27(2):252–257
20. Yang Z et al (1997) Scaphopisocapitate alignment: criterion to establish a neutral lateral view of the wrist. Radiology 205(3):865–869
21. Gilula LA (1979) Carpal injuries: analytic approach and case exercises. AJR Am J Roentgenol 133(3):503–517
22. Peh WC, Gilula LA (1996) Normal disruption of carpal arcs. J Hand Surg Am 21(4):561–566
23. Schimmerl-Metz SM et al (1999) Radiologic measurement of the scapholunate joint: implications of biologic variation in scapholunate joint morphology. J Hand Surg Am 24(6):1237–1244
24. Metz VM et al (1993) Wide scapholunate joint space in lunotriquetral coalition: a normal variant? Radiology 188(2):557–559
25. Gilula LA, Weeks PM (1978) Post-traumatic ligamentous instabilities of the wrist. Radiology 129(3):641–651
26. Moneim MS (1981) The tangential posteroanterior radiograph to demonstrate scapholunate dissociation. J Bone Joint Surg Am 63(8):1324–1326

27. Lawand A, Foulkes GD (2003) The "clenched pencil" view: a modified clenched fist scapholunate stress view. J Hand Surg Am 28(3):414–418; discussion 419–420
28. Schernberg F (1990) Roentgenographic examination of the wrist: a systematic study of the normal, lax and injured wrist. Part 1: the standard and positional views. J Hand Surg Br 15(2):210–219
29. Meade TD, Schneider LH, Cherry K (1990) Radiographic analysis of selective ligament sectioning at the carpal scaphoid: a cadaver study. J Hand Surg Am 15(6):855–862
30. Theumann NH et al (2006) Association between extrinsic and intrinsic carpal ligament injuries at MR arthrography and carpal instability at radiography: initial observations. Radiology 238(3):950–957
31. Dao KD et al (2004) The efficacy of ultrasound in the evaluation of dynamic scapholunate ligamentous instability. J Bone Joint Surg Am 86-A(7):1473–1478
32. Finlay K, Lee R, Friedman L (2004) Ultrasound of intrinsic wrist ligament and triangular fibrocartilage injuries. Skeletal Radiol 33(2):85–90
33. Griffith JF et al (2001) Sonography of the normal scapholunate ligament and scapholunate joint space. J Clin Ultrasound 29(4):223–229
34. Jacobson JA et al (2002) Sonography of the scapholunate ligament in four cadaveric wrists: correlation with MR arthrography and anatomy. AJR Am J Roentgenol 179(2):523–527
35. Ahn JM et al (1998) Evaluation of the triangular fibrocartilage and the scapholunate and lunotriquetral ligaments in cadavers with low-field-strength extremity-only magnet. Comparison of available imaging sequences and macroscopic findings. Invest Radiol 33(7):401–406
36. Anderson ML et al (2008) Diagnostic comparison of 1.5 Tesla and 3.0 Tesla preoperative MRI of the wrist in patients with ulnar-sided wrist pain. J Hand Surg Am 33(7):1153–1159
37. Lenk S et al (2004) 3.0 T high-resolution MR imaging of carpal ligaments and TFCC. Rofo 176(5):664–667
38. Saupe N et al (2005) MR imaging of the wrist: comparison between 1.5- and 3-T MR imaging—preliminary experience. Radiology 234(1):256–264
39. Magee T (2009) Comparison of 3-T MRI and arthroscopy of intrinsic wrist ligament and TFCC tears. AJR Am J Roentgenol 192(1):80–85
40. Berger RA (1996) The gross and histologic anatomy of the scapholunate interosseous ligament. J Hand Surg Am 21(2):170–178
41. Sokolow C, Saffar P (2001) Anatomy and histology of the scapholunate ligament. Hand Clin 17(1):77–81
42. Ritt MJ et al (1998) Lunotriquetral ligament properties: a comparison of three anatomic subregions. J Hand Surg Am 23(3):425–431
43. Ritt MJ et al (1998) The lunotriquetral joint: kinematic effects of sequential ligament sectioning, ligament repair, and arthrodesis. J Hand Surg Am 23(3):432–445
44. Moser T et al (2008) Multidetector CT arthrography of the wrist joint: how to do it. Radiographics 28(3):787–800; quiz 911
45. Maizlin ZV et al (2009) MR arthrography of the wrist: controversies and concepts. Hand (N Y) 4(1):66–73
46. Moser T et al (2007) Wrist ligament tears: evaluation of MRI and combined MDCT and MR arthrography. AJR Am J Roentgenol 188(5):1278–1286